

A Simple MPPT Based Control Strategy Applied to a Variable Speed Squirrel Cage Induction Generator

¹H. Merabet Boulouiha, ¹A. Tahri, ¹A. Allali, ²A. Draou and ³M. Denai

¹*Department of Electrical Engineering, University of Science and Technology of Oran, Algeria.*

²*Department of Electrical and Electronic, University of Hail, Kingdom of Saudi Arabia.*

³*School of Science and Engineering, Teesside University, TS1 3BA, Middlesbrough, UK.*

This paper presents a comprehensive modelling and control study of a variable speed wind energy conversion system based on a squirrel-cage induction generator (SCIG). The mathematical model of the SCIG is derived in Park frame along with the indirect field oriented control (IFOC) scheme based on a Proportional and Integral (PI) speed controller. A simple Maximum Power Point Tracking (MPPT) strategy is used to determine the optimal speed under variable wind speed conditions which is then used as the reference in the IFOC scheme. Power flow between the supply and the inverter is regulated via simultaneous control of the active and reactive currents of the grid and the DC link voltage. To simplify the logic software and reduce hardware requirements, a programmed PWM based on a look-up table is used to control the inverter switches. The overall model structure is implemented using MATLAB/SIMULINK and SimPowerSystems toolbox. The simulation results show that the proposed control technique is able to maximise the energy extracted from the wind during the simulation scenarios considered. The results also demonstrate good transient response characteristics in the decoupled real and reactive powers.

1. INTRODUCTION

In last recent years, renewable sources of energy have experienced considerable developments due to the increase in energy needs, decline in fossil fuel resources and the world concerns on environmental impacts and climate change. Wind energy is among the fastest-growing renewable energy technologies today and the penetration of wind power production into electric grid is rapidly increasing¹. Wind turbine configurations using various types of generators have been studied extensively and are still the subject of active research². Among the electrical machinery technology used for the conversion of wind energy, the squirrel-cage induction generator offers the advantages of high reliability, low maintenance requirements and cost, and is very light³. Doubly-fed

induction generators (DFIG) have also been very popular in variable-speed wind turbine configurations^{2,3}. Recently, permanent magnet synchronous generator (PMSG) have received much attention in wind power generation because of advantages such as self-excitation capability, better reliability, lower maintenance, and higher efficiency⁴⁻⁶. The amount of power that can be generated from a wind energy conversion system depends on several parameters such as the wind speed and the geographical location. MPPT allow variable-speed wind turbine to operate at an optimal rotation speed as a function of wind speed and capture the maximum power from the available wind energy. Many different MPPT control strategies have been developed for variable speed wind energy conversion system^{7,8}. The MPPT method used in this work is based on the knowledge of the wind turbine characteristic. Points of maximum power for the turbine's MPPT are stored in look-up table. The MPPT output is the optimum velocity which varies according to the captured wind speed. This optimal velocity will be used as the reference of the IFOC strategy of the induction generator. The control design of the system is obtained by pole placement method. The PWM technique requires a programmed control law for the side inverter and the DC link voltage based on the input which are the modulation index in amplitude (MI) and phase angle (α). The programmed PWM technique, developed and implemented as a look up table (different from the MPPT look-up-table), is used to control the six inverter switches. The programmed PWM has the following advantages: It allows approximately 50% reduction in the switching frequency compared to conventional sinusoidal PWM. A high gain voltage due to over-modulation can be achieved. Inverters DC side current is lower because of the high quality of the inverter's output voltage and current of the inverter. Reducing the PWM switching frequency reduces the switching losses of the inverter which can therefore be used for high power applications. The look up table of the programmed PWM technique is used to control the DC side voltage and the active and reactive currents. The reference of the reactive current is set to zero to ensure power flow to the supply with a unity power factor.

In this paper, a mathematical model of the SCIG is derived in Park frame in order to design the indirect field oriented control (IFOC) based speed control. The simulation is carried out under MATLAB/SIMULINK and SimPowerSystems toolbox.

The rest of the paper is organised as follows: Section 2 introduces the overall simulation model structure and develops the relevant control strategies for the MPPT and SCIG. Section 3 of the paper presents the modelling and control of the DC side and grid. Finally, the simulation results and conclusions are summarised in Section 4 and 5 respectively. Appendix A includes the mathematical models of the wind turbine, SCIG and a brief description of the programmed PWM technique and the inverter..

II. DESCRIPTION OF THE SYSTEM'S MODEL

The system being modelled includes a three-bladed wind turbine connected to variable-speed SCIG as shown in FIG. 1.

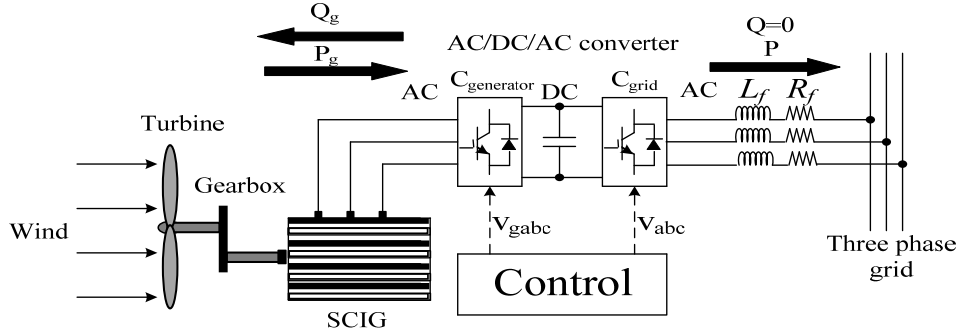


FIG. 1 Wind turbine with a squirrel-cage induction generator SCIG.

The detailed model of control of the side generator converter and the side grid converter is presented by FIG. 2.

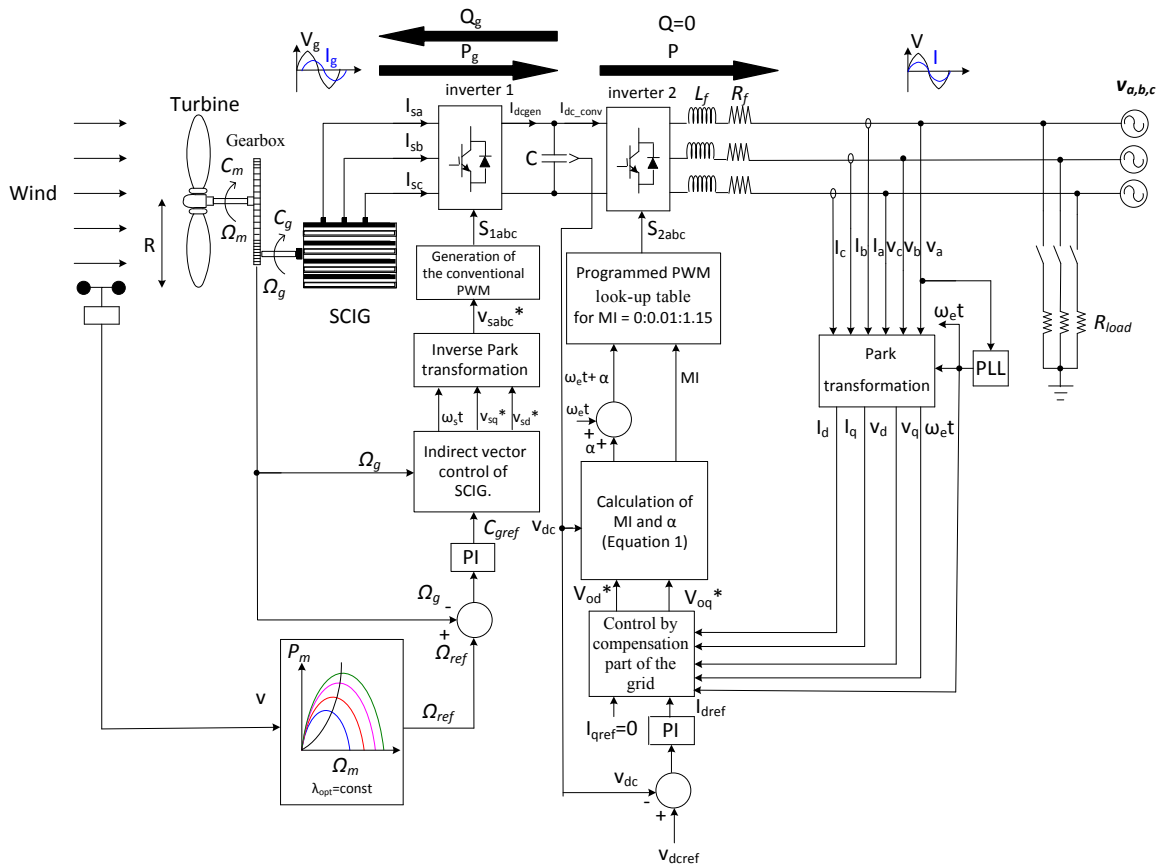


FIG. 2. Bloc diagram of the proposed circuit for controlling the SCIG.

With

$$MI = \left[\frac{\sqrt{V_{od}^2 + V_{oq}^2}}{V_{dc}} \right] \sqrt{\frac{3}{2}} \quad \text{and} \quad \alpha = \text{artg} \left[\frac{V_{oq}}{V_{od}} \right] \quad (1)$$

Where: ω_e defines the grid frequency and α is the phase shift between the fundamental component of the side grid converter voltage and the current of the grid.

The wind turbine is connected to the supply through two converters AC/DC/AC. In the generator mode, the first converter is used as a PWM rectifier which ensures current flow from the induction generator AC side to the DC side. The reference of the DC bus voltage is chosen to be greater than the forward voltage on the grid side to ensure the passage of the power generated by the induction generator to the grid. The grid side converter is used for controlling the DC side voltage magnitude and the active and reactive powers by adjusting the modulation index (MI) of the inverter and the phase shift (α) between the voltage and current components of the grid. The control system requires the voltages and currents on the source side as well as the DC side voltage magnitude. The AC voltages and currents are transformed into d-q components when their frequency coincides with the grid frequency hence a phase locked loop circuit is used to determine the phase of the grid.

The models of the wind turbine, SCIG and programmed PWM inverter are detailed in Appendix A.

A. The MPPT Strategy

Depending on the wind aerodynamic conditions, there exists an optimal operating point which may allow the extraction of maximum power from the turbine. The power captured by the wind turbine (equation (A.1)) can be substantially maximized by adjusting the coefficient C_p which represents the aerodynamic efficiency of the wind turbine and is dependent on the speed of the generator (or the speed ratio λ). It is necessary to design control strategies to maximize the power generated (thus the torque) by adjusting the speed of the turbine to a reference value regardless of the disturbances acting on the wind speed. There are different methods to adjust wind turbine at partial load following the trajectory of maximum power MPPT. Two different controllers been considered, the indirect speed controller speed (ISC) and direct speed controller (DSC). Thus, we have to control either the rotational speed of the turbine or the power of the turbine to reach this point. There are several MPPT methods in the literature: Those which are not based on the knowledge of the wind turbine characteristic (direct methods) and those which use the wind turbine characteristic (indirect methods). Direct methods usually lead to a complex control structure depending on the approach used to search for the MPPT. Indirect method, such as the one used in this work, searches for a pseudo maximum power point from the knowledge of the characteristic curve of the wind turbine to be driven. These methods move rapidly towards the optimum using simple measures and the internal mechanical-electrical converter, in other words, without the need to capture the wind speed. This process requires the constructor to perform a set of wind characterization tests (external fan) or

simulations of blade profile. For this reason, most of wind energy systems implementing an MPPT strategy are based on the knowledge of the turbine characteristics.

The optimum angular speed $\Omega_{m, opt}$ for the mechanical transmission of the maximum wind turbine is given by:

$$\Omega_{m, opt} = \frac{\lambda_{opt} v}{R} \quad (2)$$

The following relation can be deduced:

$$P_{m, max} = K_{p, opt} \Omega_{m, opt}^3 \quad (3)$$

Where

$$K_{p, opt} = \frac{1}{2} \rho C_{p, max} \frac{R^5}{\lambda_{opt}^3} \quad (4)$$

Thus, the corresponding optimum torque is:

$$C_{m, opt} = \frac{P_{m, max}}{\Omega_{m, opt}} = K_{p, opt} \Omega_{m, opt}^2 \quad (5)$$

The power characteristic of the turbine is shown in FIG. 3. Note that this characteristic is generated using equations (3) and (A1). The locus of the point representing the maximum power can be determined and tracked by adapting the speed of the turbine (thick curve). Thus, to maximize the converted power, the turbine speed must be adapted to wind speed¹⁰.

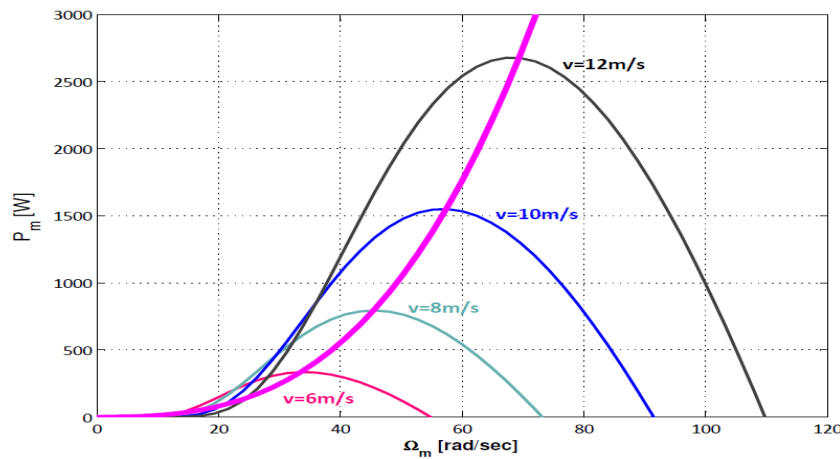


FIG. 3. Optimum operating characteristics of the turbine.

The electric power supplied by the machine resulting from electromechanical conversion, is directly induced by the speed of rotation imparted to its input. That is why it is advantageous to insert between rotor of the machine and the helix of the wind, a multiplier. This multiplier may be modeled as a gain G , and chosen to maintain the

generator axis speed within a desired range. Neglecting transmission loss, the torque and speed of the axis wind turbine, referred to the side of the generator transmission (i.e. multiplier) are given by:

$$C_g = \frac{C_m}{G}, \quad \Omega_m = \frac{\Omega_g}{G} \quad (6)$$

Where G represents a gain of the multiplier

B. Indirect Vector Control of the SCIG

Vector control or Field oriented control (FOC) consists of controlling independently the flux and torque by the d- and q-components of the current respectively. If the d-q reference frame is linked to the rotating field with an orientation of the rotor flux (d-axis aligned with the direction of the rotor flux), then:

$$\Phi_{rd} = \Phi_r, \quad \Phi_{rq} = 0 \quad (7)$$

In this approach, the reference axis of the rotating armature is aligned with rotor flux vector, Φ_r ($\Phi_{rq}=0$). Under these conditions, the component current of the q-axis stator, i_{sq} , define the electrical torque of the machine component d-axis current i_{sd} , the module sets the rotor flux of the machine, similarly to a separately excited DC machine.

If the flux is kept constant, the developed torque given in (A.10) becomes:

$$C_{em} = p \frac{3}{2} \frac{L_m}{L_r} \Phi_r i_{sq} \quad (8)$$

FIG. 4 shows the block diagram of the rotor indirect field oriented control strategy of the variable speed induction generator.

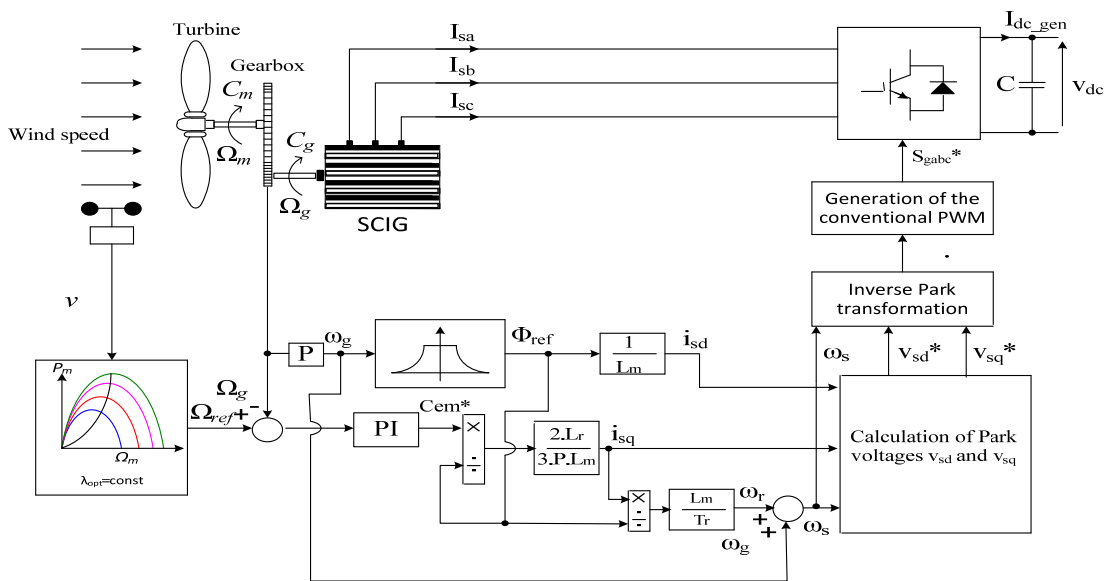


FIG. 4. Indirect vector control of the induction machine.

The speed controller is used to determine the electromagnetic torque reference. Speed may be controlled by a PI controller which is derived as described below.

With indirect vector control, the induction machine voltages v_{sd} and v_{sq} in steady-state are:

$$\begin{cases} v_{sd} = R_s i_{sd} - \omega_s L_s \sigma i_{sq} \\ v_{sq} = \omega_s L_s i_{sd} + R_s i_{sq} \end{cases} \quad (9)$$

With σ being the dispersion coefficient of Blondel defined as:

$$\sigma = 1 - \frac{L_m^2}{L_s L_r} \quad (10)$$

And the steady-state value of the flux becomes:

$$\Phi_r = L_m i_{sd} \Rightarrow i_{sd} = \frac{\Phi_r}{L_m} \quad (11)$$

The transfer function of the mechanical speed of the induction generator is given by:

$$\frac{\Omega_g}{C_{em}} = \frac{1}{Js + f} = \frac{1/J}{s + f/J} = \frac{g_\Omega}{s + p_\Omega} \quad (12)$$

Where $g_\Omega = 1/J$ and $p_\Omega = f/J$ are respectively the static gain and the pole of the transfer function of the mechanical speed of the asynchronous generator.

The closed-loop transfer function is:

$$G_{BF}(s) = \frac{g_\Omega [K_{p\Omega} s + K_{i\Omega}]}{s^2 + [g_\Omega K_{p\Omega} + p_\Omega] s + g_\Omega K_{i\Omega}} \quad (13)$$

The controller parameters can be determined using pole placement. Let the desired closed-loop poles be:

$$s_{1,2} = -\sigma_c \pm j\omega_n \sqrt{1 - \xi^2} = \gamma(-1 \pm j) \quad (14)$$

The poles are selected to improve the closed-loop response by three-fold with regard to the open-loop system. Solving for the PI controller's parameter:

$$\begin{cases} K_{p\Omega} = \frac{2\gamma - p_\Omega}{g_\Omega} = 2\gamma J - f \\ K_i = \frac{2\gamma^2}{g_\Omega} = 2\gamma^2 J \end{cases} \quad (15)$$

III. CONTROL OF THE DC SIDE AND THE GRID

The DC side circuit in the Park's coordinate system is modeled as:

$$\frac{d}{dt} \begin{bmatrix} i_d \\ i_q \end{bmatrix} = \begin{bmatrix} -\frac{R_f}{L_f} & \omega_e \\ -\omega_e & -\frac{R_f}{L_f} \end{bmatrix} \begin{bmatrix} i_d \\ i_q \end{bmatrix} + \frac{1}{L_f} \begin{bmatrix} v_d - v_{od} \\ v_q - v_{oq} \end{bmatrix} \quad (16)$$

Where ω_e is the pulsating frequency of the grid, v_d and v_q are the source voltages and v_{od} and v_{oq} represent the inverter voltages.

By using the decoupling method by compensation, the inverter voltages can be written as:

$$\begin{cases} v_{od} = e_{od} - v_{od1} \\ v_{oq} = e_{oq} - v_{oq1} \end{cases} \quad (17)$$

With the control coefficients:

$$\begin{cases} v_{od1} = L_f s i_d \\ v_{oq1} = L_f s i_q \end{cases} \quad (18)$$

And the coefficients of compensation are obtained as:

$$\begin{cases} e_{od} = -R_f i_d + L_f \omega_e i_q + v_d \\ e_{oq} = -L_f \omega_e i_d - R_f i_q + v_q \end{cases} \quad (19)$$

The DC bus voltage v_{dc} varies with the power exchanged between the turbine and the grid and is given by:

$$C \frac{dv_{dc}}{dt} = I_{dc} = I_{dc_gen} - I_{dc_conv} \quad (20)$$

The Park transformation to the side of the grid is based on a reference linked to the rotating field of the grid. In this approach, the d axis is aligned with the voltage grid vector, therefore the q-axis component of the voltage is zero ($v_q = 0$). In this case, the active and reactive powers can be written as:

$$\begin{cases} P = \frac{3}{2} v_d i_d \\ Q = -\frac{3}{2} v_d i_q \end{cases} \quad (21)$$

The active power transmitted by the DC link can be expressed as:

$$P_{dc} = v_{dc} I_{dc} \quad (22)$$

The power transferred through the DC side should be equal to the power transferred to the grid.

$$P_{dc} = P \Rightarrow v_{dc} I_{dc} = \frac{3}{2} v_d i_d \quad (23)$$

The grid side inverter is used to control voltage of capacitor and continuous link currents of the d-axis and q Park grid.

The proposed control strategy for the DC link is depicted in FIG. 5. It contains two control loops, an inner loop and an outer loop. The outer loop consists of a PI controller for controlling the voltage of the DC link. The output of the DC voltage controller is the reference d-axis current i_{dref} from the grid to be compared with the measured current I_{dmeas} . The quadrature component of the grid current i_q is used to control the flow of reactive power. Here, the reactive power reference is set to zero in order to obtain a unity power factor.

The reference voltage for the DC side v_{dref} is generally set larger than the voltage v_d of the grid. For a grid voltage of $v_s = 380$ V (that is to say $v_d = \sqrt{2/3}v_s$), we set the reference voltage for the DC link $v_{dref} = 800$ V.

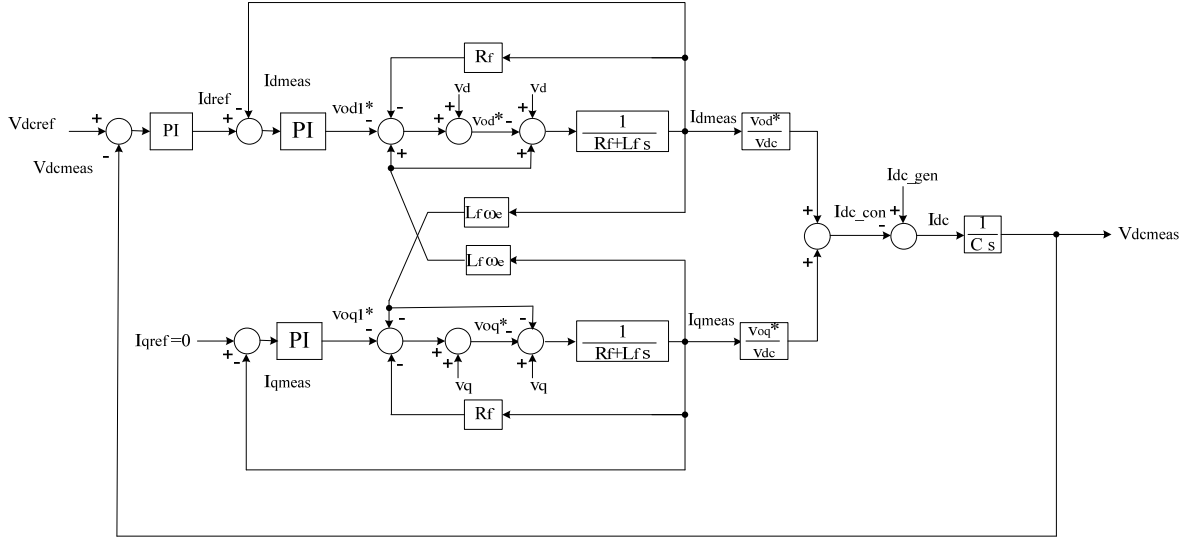


FIG. 5. Block diagram for the control of the grid currents and DC bus voltage.

The continuous DC link voltage is maintained at a fixed value while the grid side inverter controls the active power flow so that the power developed is transferred to the grid. This is the reason why the controller of the DC link output voltage determines the reference for the d-axis current of the grid. The reference of the q-axis current of the grid is adjusted zero to have a unity power factor. Decoupling is applied to the two control loops of the grid currents to achieve independent control of the d and q current components.

IV. SIMULATION RESULTS

The parameters values of all the components used in the simulation are listed in the Appendix B (Table B.1 and Table B.2).

FIG. 6 shows the active and reactive powers and phase voltages of the generator. Before the time of the action of the wind turbine, we note that the active power reaches a low value representing the iron and copper losses of the generator. At the time of the action of the wind turbine at $t=0.3$ sec, we notice that the generator provides an active power equal to - 2 kW for a wind velocity of $v=12$ m/sec. For a change of wind speed ($v=10$ m/sec) at time $t=0.8$ sec, there is a fall of almost half the active power (that is to say $P_g \approx -1$ kW). The active power returns to its rated value of -2 kW for a wind velocity of $v=12$ m/sec at $t=1.4$ sec.

The reference power P_{ref} is obtained via the MPPT strategy according to the wind speed available. Note that, based on the characteristic of the wind turbine in FIG. 3, each wind speed corresponds a given reference power. For instance, for a speed of 12m/sec is associated with a reference power of -2kW.

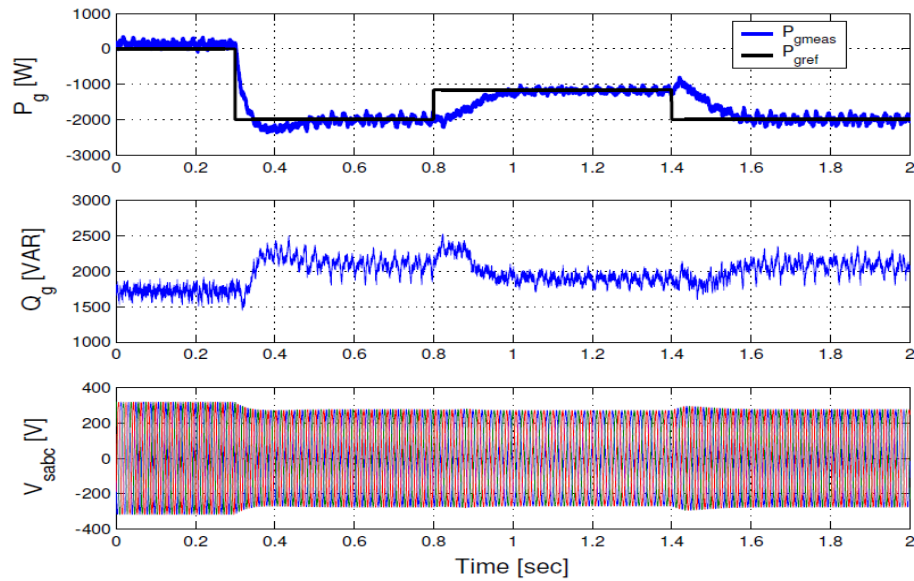


FIG. 6. Generator active and reactive power and three phase stator voltage.

FIG. 7 shows the wind speed, the speed and the electromagnetic torque and the three-phase stator currents of the generator for the same changes in wind characteristics. In this result, the turbine was subjected to a disturbance simulated as an increase or reduction in the wind speed (see FIG. 7). The speed is continuously monitored according to the reference of the wind speed captured. The voltage waveform and power are shown in FIG. 8. It can be noted that the DC voltage reference is maintained at 800 V after a short transient despite changes in wind speed from 12 m/sec to 10 m/sec. The power and current of the DC side is almost zero in steady state. The responses of the grid active and reactive power and waveforms of grid phase currents and load are illustrated in FIG. 9.

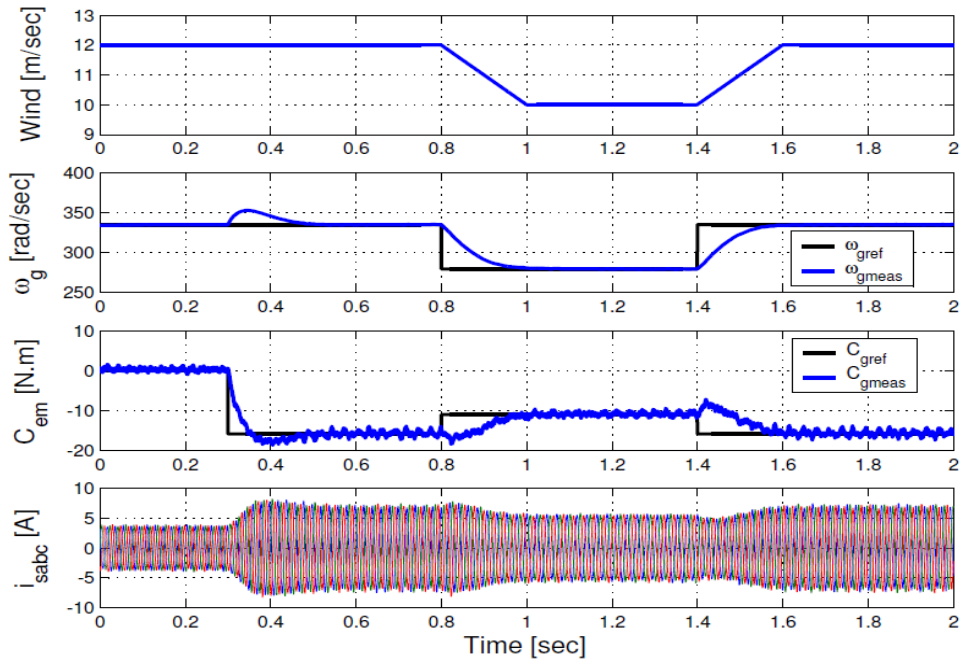


FIG. 7. Wind speed, generator angular velocity, electromagnetic torque and three-phase currents.

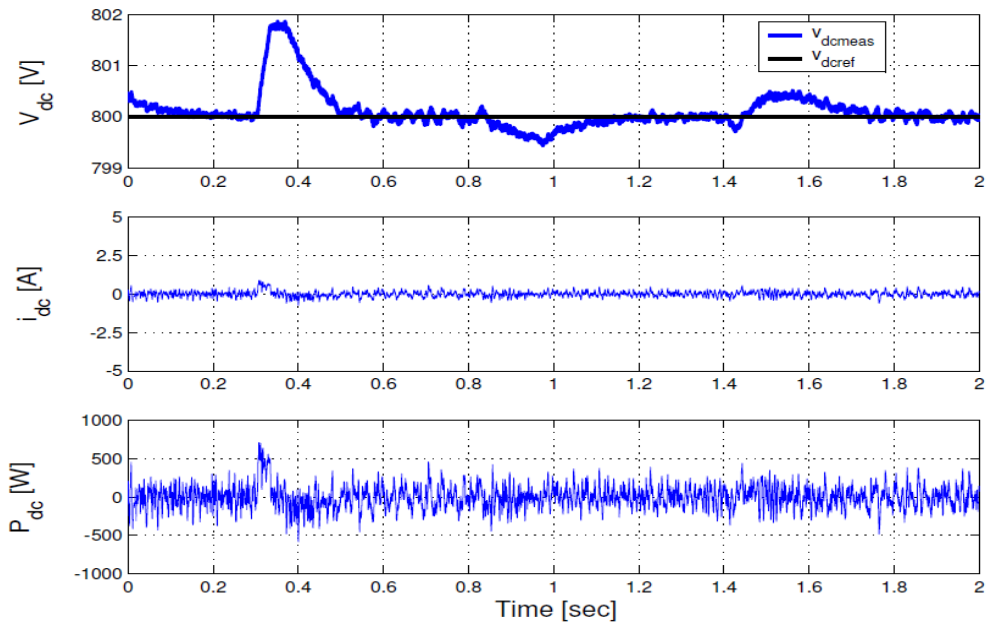


FIG. 8. DC link voltage, current and Power waveforms.

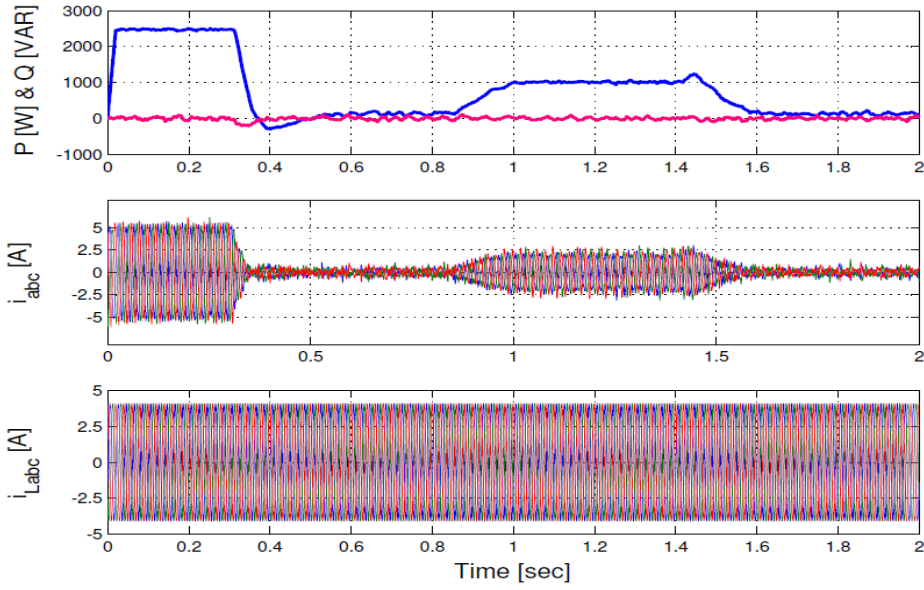


FIG. 9. Active and reactive power of the grid, grid and load phase currents.

Before the intervention of the wind turbine, we note that the source must supply an active power to the load and the losses of the generator, but at the time of the operation of the turbine for $v = 12$ m/sec the power of the grid is expected to be near zero by the generator that provided the necessary power (-2 kW) to supply the load. In the case of change of wind, the generator provided only half of that power thus forcing its source to provide the other half of the power required by the load.

FIG. 10 shows the Park current with three-phase voltages of the grid for the same change of wind. The constant direct current i_d follows its waveform obtained by the voltage regulator. Similarly, for the quadratic current i_q but only the reference of this current is zero. The power coefficient C_p and the tip speed ratio λ are plotted in FIG. 11; As expected, the power coefficient C_p is maintained at an optimal value of 0.411 after a short transient while the speed λ settles at a the maximum value of 8.

FIG. 12 shows the responses of voltage, phase angle and amplitude modulation index of the grid side. The phase shift α controls the power flow between the side grid converter and the grid. Since the reference for reactive current component is set to zero, therefore the α phase is almost zero. On the other hand, the control of the grid active power and the voltage level of DC link are performed via the amplitude modulation index MI. It can be noted that MI changes when the wind speed is stepped from 12m/sec to 10m/sec and back to 12m/sec.

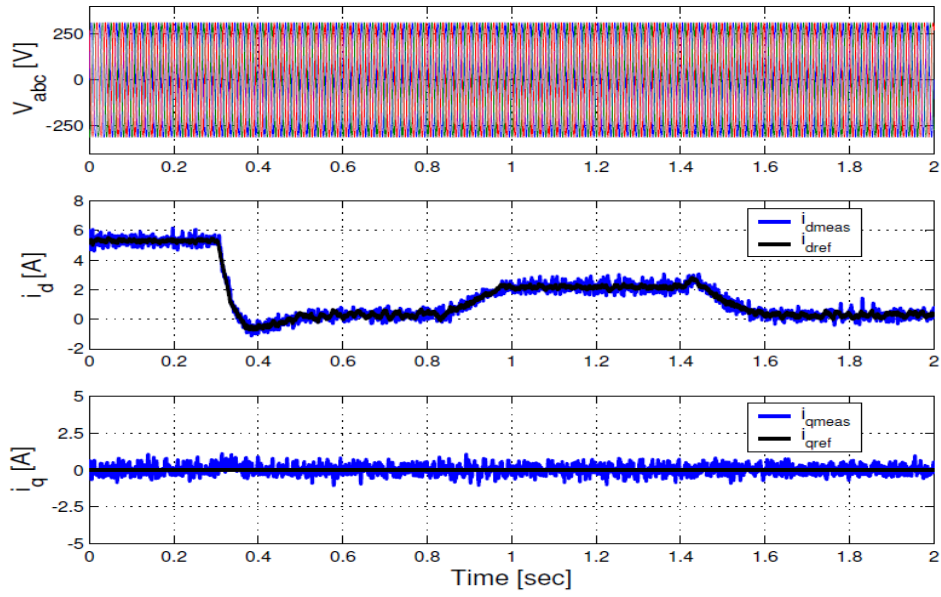


FIG. 10. Three phase voltage and the grid side quadrature component of the current.

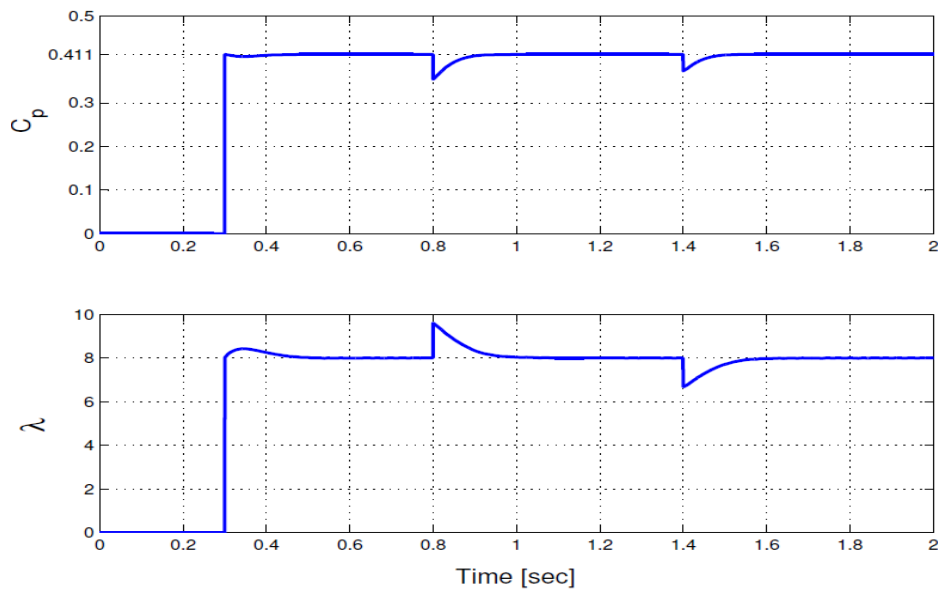


FIG. 11. Responses of the power coefficient C_p and tip speed ratio λ .

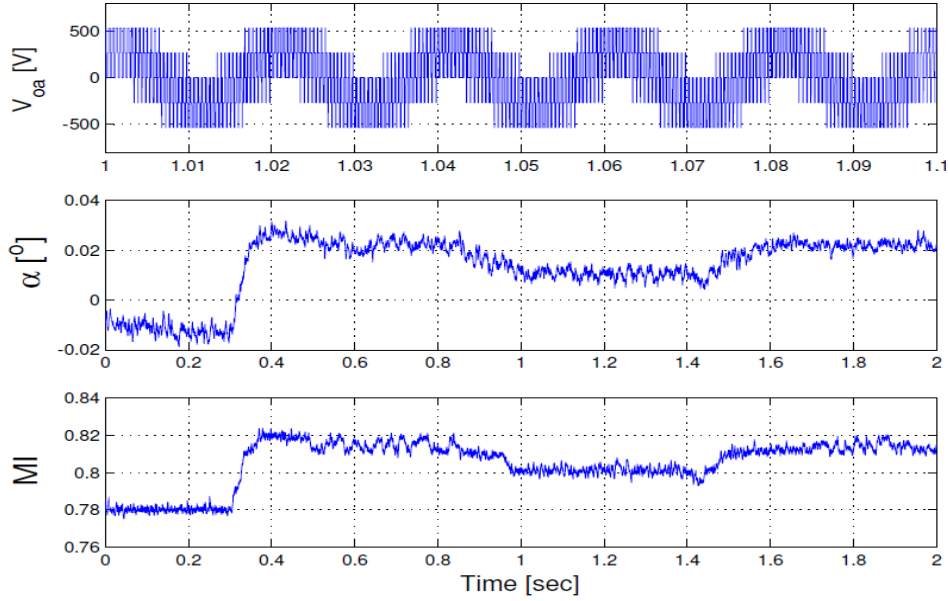


FIG 12. Voltage of the inverter and phase and modulation index of the side grid amplitude.

V. CONCLUSION

The paper proposes a SCIG-based variable speed wind energy conversion system with a simple MPPT control strategy based on the knowledge of the wind turbine characteristics. The PI controllers for the DC side voltage as well as the direct and quadrature current components in the grid side have been designed using a simple pole placement technique. The grid quadratic current component I_q is used to modulate the flow of reactive power. In our case, the reactive power reference is set to zero, to obtain a unity power factor. The switching signals for the grid side three-phase inverter, which controls the DC voltage level, the direct current component (i_d for controlling the active power of the grid) and the quadratic current component (i_q for the reactive power flow), are obtained via a programmed PWM technique, this has reduced the level of harmonics in the output waveforms. Simulation results show the effectiveness of the overall proposed control strategy. The control system was able to maximise the energy extracted from the wind as reflected from the power coefficients obtained during the simulation scenarios considered. The results also demonstrate good transient response characteristics in the decoupled real and reactive powers. As future work, the authors believe that the results can improved through the design of faster and more robust multivariable controllers. Direct torque control (DTC) can also be used to control the speed and torque as it has proved more effective than IFOC in the terms of energy quality since DTC does not depend on the generator parameters.

REFERENCES

- ¹ R. Rechsteiner, "Wind Power in Context - A Clean Revolution in the Energy Sector," 2008.
- ² H. Sik Kim, D. Dah-Chuan Lu, "Wind Energy Conversion System from Electrical Perspective - A Survey," *Smart Grid and Renewable Energy* **1**, 119 (2010).
- ³ H. An, H. Ko, H. Kim, H. Kim, S. Kim, G. Jang, B. Lee, "Modeling and Voltage-Control of Variable-Speed SCAG-Based Wind Farm", *Renewable Energy* **42**, 28 (2012).
- ⁴ M. Lindholm "Doubly Fed Drives for Variable Speed Wind Turbine – A 40 kW Laboratory Setup" Ph.D thesis, Technical University of Denmark, (2004).
- ⁵ C. N. Bhende, S. Mishra and S. G. Malla Tanaka, "Permanent Magnet Synchronous Generator-Based Standalone Wind Energy Supply System," *IEEE Transactions on Sustainable Energy* **2(4)**, 361 (2011).
- ⁶ M. E. Haque, M. Negnevitsky, and K. M. Muttaqi, "A Novel Control Strategy for a Variable-Speed Wind Turbine with a Permanent-Magnet Synchronous Generator," *IEEE Trans. Ind. Appl.* **46(1)**, 331 (2010).
- ⁷ G.D. Moor and H.J. Beukes, "Maximum Power Point Trackers for Wind Turbines," *Power Electronics Specialist Conference (PESC)*, 2044 (2004).
- ⁸ M.A. Abdullah, A.H.M. Yatim, C.W. Tan and R. Saidur, "A Review of Maximum Power Tracking Algorithms for Wind Energy Systems," *Renewable and Sustainable Energy Reviews* **6(5)**, 3220 (2012).
- ⁹ H. S. Patel, and R. G. Hoft, "Generalized of Harmonic Elimination and Voltage Control in Thyristor Inverters Part I-Harmonic Elimination, *IEEE Trans. Ind. Appl.* Vol. IA-9, pp.310-317, May/June 1973.
- ¹⁰ A. Davigny, "Participation aux Services Système de Fermes d'Eoliennes à Vitesse Variable Intégrant du Stockage Inertiel d'Énergie," Thèse de Doctorat, Université de Lille, (2007).
- ¹¹ C.K. Rai, "Non Conventional Energy Sources of Energy, Khanna Publishers, New Delhi, 1996.
- ¹² Y. Lei, A. Mullane, G. Lightbody and R. Yacamini "Modeling of the Wind Turbine with a Doubly Fed Induction Generator for Grid Integration Studies," *IEEE Transactions on Energy Conversion* **21(1)**, 257 (2006).
- ¹³ A. Kuperman, R. Rabinovici and G. Weiss, "A shunt connected inverter based variable speed wind turbine generation," *Int. Jour. of Electromotion* **13(1)**, 67 (2006).
- ¹⁴ R. Gagnon, B. Saulnier, G. Sybille, P. Giroux, "Modeling of a Generic High-Penetration No-Storage Wind-Diesel System Using Matlab/Power System Blockset," *Global Windpower Conference*, Paris, France, April (2002).
- ¹⁵ E. Muljadi, C. P. Butterfield, "Pitch-Controlled Variable Speed Turbine Generation", *IEEE Trans. Ind. Appl.*, **37(1)**, 240 (2001).
- ¹⁶ Lanzafame R, Messina M. "Fluid Dynamics Wind Turbine Design: Critical Analysis, Optimization and Application of BEM Theory," *Renewable Energy* **32(14)**, 2291 (2007).
- ¹⁷ F. Poitiers, T. Bouaouiche, M. Machmoum, "Advanced Control of Doubly-Fed Induction Generator for Wind Energy Conversion," *Electric Power Systems Research* **79 (7)**, 1085 (2009).
- ¹⁸ G. Saccomando, J. Svensson, A. Sannino, "Improving Voltage Disturbance Rejection for Variable-Speed Wind Turbines," *IEEE Trans. on En. Conv.* **17(3)**, 422 (2002).
- ¹⁹ T. Sun, Z. Chen, F. Blaabjereg, "Flicker Study on Variable Speed Wind Turbines with Doubly-Fed Induction Generators," *IEEE Trans. on En. Conv.* **20(4)**, 896 (2005).
- ²⁰ E. Tremblay, A. Chandra, P.J. Lagacé, "Grid Side Converter Control of DFIG Wind Turbines to Enhance Power Quality of Distributed Network," in: *IEEE Power Engineering Society General Meeting* 1, 118 (2006).

APPENDIX A

A.1) Wind Turbine Model

The relationship between the wind speed and the mechanical aerodynamic transmission extracted from the wind can be described as follows¹¹⁻¹⁵.

$$P_m = \frac{1}{2} \rho \cdot \pi \cdot R^2 \cdot C_p(\lambda, \beta) \cdot v^3 \quad (\text{A.1})$$

Where $P_m [W]$ is the mechanical power of the wind turbine and $\beta [^\circ]$ represents the orientation angle of the blades. The power coefficient C_p defines the aerodynamic efficiency of the wind turbine. It depends on the characteristic of the turbine and is a function of speed ratio λ and the orientation angle β of the blade.

$$C_p(\lambda, \beta) = C_1 \left(\frac{C_2}{\lambda_i} - (C_3 + C_4) \beta - C_5 \right) e^{-\frac{C_6}{\lambda_i}} \quad (\text{A.2})$$

The values of C_1 - C_6 (Table A.I) were chosen based on the BEM method (Blade Element Momentum)¹⁶:

TABLE A.I. Coefficients of the turbine for obtaining the power coefficient.

C_1	C_2	C_3	C_4	C_5	C_6
0.5	33	0.2	0	0.4	12.7

With

$$\frac{1}{\lambda_i} = \frac{1}{\lambda + 0.08\beta} - \frac{0.035}{\beta^3 + 1} \quad (\text{A.3})$$

λ is defined as the ratio of the linear velocity at the end of the blade and the wind speed of the free jet and is given by¹⁷⁻²⁰:

$$\lambda = \frac{\Omega_m R}{v} \quad (\text{A.4})$$

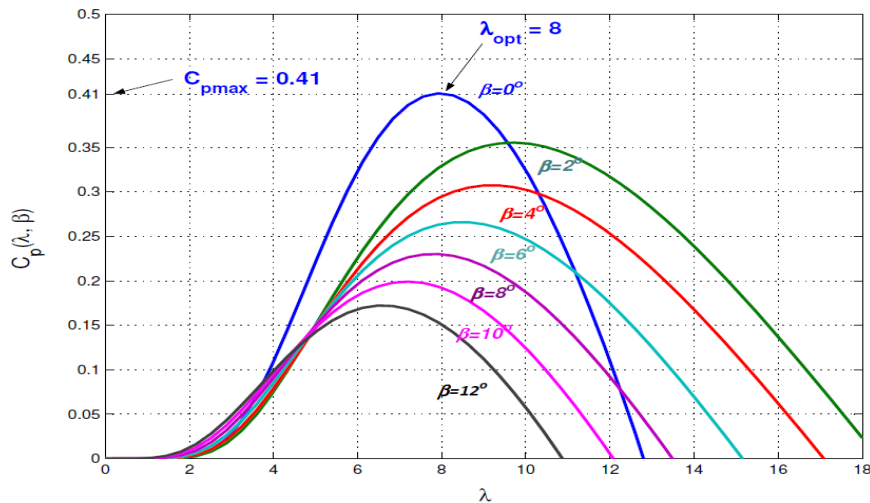


Fig. A.1. Characteristic of the power coefficient as a function of λ .

It can be seen from FIG. A.1 that the power coefficient reaches a maximum for a orientation angle of the blades of 0° and a particular value of the velocity ratio which is known as λ_{opt} (where $\lambda_{opt} = 8$), and a power coefficient corresponding to λ_{opt} which is $C_{pmax} = 0.411$.

A.2) Model of the SCIG

Based on the equivalent circuit of induction machine in the Park system, shown in Fig. A.2, the following equations can be written:

- For the two-phase equivalent stator winding

$$\begin{cases} v_{sd} = R_s i_{sd} - \omega_s \Phi_{sq} + \frac{d\Phi_{sd}}{dt} \\ v_{sq} = R_s i_{sq} + \omega_s \Phi_{sd} + \frac{d\Phi_{sq}}{dt} \end{cases} \quad (\text{A.5})$$

Where v_{sd} v_{sq} are the stator voltage components in the Park system, ω_s is the synchronous speed of the generator and Φ_{sd} Φ_{sq} i_{sd} i_{sq} are respectively the flux and the stator current components in d and q axis of Park frame.

- For the two-phase equivalent rotor winding

$$\begin{cases} v_{rd} = 0 = R_r i_{rd} - \omega_r \Phi_{rq} + \frac{d\Phi_{rd}}{dt} \\ v_{rq} = 0 = R_r i_{rq} + \omega_r \Phi_{rd} + \frac{d\Phi_{rq}}{dt} \end{cases} \quad (\text{A.6})$$

The rotor voltages v_{rd} and v_{rq} are set to zero for a short-circuited rotor. ω_r is the rotor speed of the generator and Φ_{rd} Φ_{rq} i_{rd} i_{rq} are respectively the flux and the d-q rotor current components.

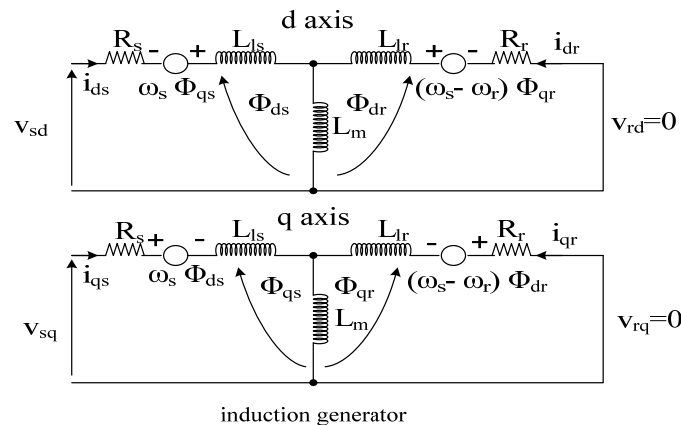


FIG. A.2. Equivalent circuit of Induction Machine.

The model's flux vectors and currents in the d- q system are:

- Stator:

$$\begin{cases} \Phi_{sd} = L_s i_{sd} + L_m i_{rd} \\ \Phi_{sq} = L_s i_{sq} + L_m i_{rq} \end{cases} \quad (\text{A.7})$$

- Rotor:

$$\begin{cases} \Phi_{rd} = L_m i_{sd} + L_r i_{rd} \\ \Phi_{rq} = L_m i_{sq} + L_r i_{rq} \end{cases} \quad (\text{A.8})$$

And the mechanical equation is:

$$C_{em} - C_m = f \Omega_g + J \frac{d\Omega_g}{dt} \quad (\text{A.9})$$

Where C_{em} is the electromagnetic torque [N.m] and C_m denotes the mechanical torque produced by the turbine [N.m].

The electromagnetic torque is:

$$C_{em} = p \frac{3}{2} \frac{L_m}{L_r} (\Phi_{rd} I_{sq} - \Phi_{rq} I_{sq}) \quad (\text{A.10})$$

A.3) Model of Programmed PWM Inverter

The converter is modeled at two levels with ideal switches which permit the flow of current in both directions.

The inverter line-to-line voltages are:

$$\begin{cases} V_{ab} = V_{ao} - V_{bo} \\ V_{bc} = V_{bo} - V_{co} \\ V_{ca} = V_{co} - V_{ao} \end{cases} \quad (\text{A.11})$$

V_{ao} , V_{bo} and V_{co} being the input voltages of the inverter or DC voltages. They are referenced to a midpoint "o" of a shadow input divider. Also, in order to calculate the inverter phase voltage (V_{an}, V_{bn}, V_{cn}), V_{no} is calculated as

$$V_{no} = \frac{1}{3}(V_{ao} + V_{bo} + V_{co}) \quad (\text{A.12})$$

The phase voltages are obtained as:

$$\begin{cases} V_{an} = V_{ao} - V_{no} \\ V_{bn} = V_{bo} - V_{no} \\ V_{cn} = V_{co} - V_{no} \end{cases} \quad (\text{A.13})$$

Finally the model of the inverter is:

$$\begin{cases} V_{an} = \frac{2}{3}V_{ao} - \frac{1}{3}V_{bo} - \frac{1}{3}V_{co} \\ V_{bn} = -\frac{1}{3}V_{ao} + \frac{2}{3}V_{bo} - \frac{1}{3}V_{co} \\ V_{cn} = -\frac{1}{3}V_{ao} - \frac{1}{3}V_{bo} + \frac{2}{3}V_{co} \end{cases} \quad (\text{A.14})$$

The programmed PWM look-up table was organized for 4 Kbytes ($4096 = 4 \times 1024$) points per cycle per MI. The MI was allowed to vary from 0 to 1.15 in steps of 0.01. Each MI value is represented by a table of $\omega_c t$ for a period of 0.02 sec with a sampling of 0.02/4096. The solutions obtained by the Newton-Raphson method to eliminate 10 harmonics for each MI, are stored in an array of size 4 Kbytes ($4 \times 1024 = 4096$) i.e. 4096 points per cycle. Two counters were then designed; a horizontal one to detect the MI and a vertical counter to detect the instant of time $\omega_c t + \alpha$, this will also be the start for a counting period of 0.02 sec in steps of 0.02/4096. Once the MI is found, the pointer of the second counter is fixed on the table corresponding to the MI obtained by the first counter from the instant ($\omega_c t + \alpha$) as shown in FIG. A.3. this illustration is only for phase A, the other phases B and C are shifted by $\pm 120^\circ$ respectively.

TABLE B.2. Parameters of the PI controllers.

<i>IFOC control block</i>	
Proportional gain of speed controller, $K_{p\Omega}$	1
Integral gain of the speed controller, $K_{i\Omega}$	15.872
<i>DC side</i>	
Capacitance, C [μF]	10^4
Proportional gain of DC voltage controller, K_{pdc}	2
Integral gain of DC voltage controller, K_{idc}	25
<i>Grid side control block</i>	
Proportional gain of current controller, K_{pc}	6
Integral gain of current controller, K_{ic}	681.82